Available online at www.sciencedirect.com
ScienceDirect
Journal of Crystal Growth 295 (2006) 1–6
JOURNAL OF CRYSTAL GROWTH
www.elsevier.com/locate/jcrysgro

ISOVPE MCT films grown on pure and alloyed CdTe substrates with different crystalline orientations

U. Gilabert[a,b], E. Heredia[c], A.B. Trigubó[b,c,*]

[a]*SEGEMAR, Gral. Paz 5445, Parque Tecnológico Miguelete, Edif. 14, San Martín, Buenos Aires, Argentina*
[b]*FRBA-UTN: Medrano 951, 1179 Cd Autónoma de Buenos Aires, Argentina*
[c]*CINSO-CONICET-CITEFA: Juan Bautista de La Salle 4397, B1603ALO Villa Martelli, Buenos Aires, Argentina*

Received 14 February 2006; accepted 17 July 2006
Communicated by R. James

Abstract

Epitaxial films of $Hg_{1-x}Cd_xTe$ (MCT) with $x \cong 0.2$ were grown on CdTe, $Cd_{0.96}Zn_{0.04}Te$ and $CdTe_{0.96}Se_{0.04}$ substrates by the isothermal vapor phase epitaxy (ISOVPE) technique with no mercury overpressure. The growth was accomplished in different crystallographic orientations: (1 1 1)Cd, (1 1 1)Te, (1 1 0) and (1 0 0).

The structural characterization of substrates and films was performed by X-ray diffraction (Laue technique), surface chemical etching and optical microscopy. Chemical composition analysis was performed by an electronic microprobe in the wavelength dispersive spectroscopic mode and electrical characterization by Hall effect measurements.

MCT is an important semiconductor for the manufacture of infrared detectors. The alloyed substrates have a closer lattice match with $Hg_{1-x}Cd_xTe$. Furthermore, these substrates usually have a lower dislocation density. Both facts determine a lower generation of lineal defects during growth. This fact could produce a larger carrier lifetime and, as a consequence, better electrical properties of devices. On the other hand the surface morphology of ISOVPE MCT epitaxial films only depends on the crystallographic orientation, being independent of the use of pure or alloyed substrates.
© 2006 Elsevier B.V. All rights reserved.

PACS: 68.55.−a; 72.80.Ey; 73.61.Ga; 81.05.Dz; 81.15.Kk

Keywords: A1. Characterization; A1. Etching; A1. Line defects; A1. Substrates; A3. Vapor phase epitaxy; B2. Semiconducting II–VI materials

1. Introduction

$Hg_{1-x}Cd_xTe$ (MCT) is a semiconductor with properties that makes it an almost ideal material for the manufacture of infrared detectors. Photoconductors, photodiodes, charge transfer devices and SPRITE [1] can be mentioned as possible detectors. High optical absorption coefficient, high electron mobility, low thermal generation rate and tunable band gap via composition variation [2] are some of its important properties.

An increasing interest for emission devices in the 2–5 μm range has emerged. MCT with $x > 0.3$ is a promising material for the manufacture of these devices because of its high absorption optical coefficient and high efficiency for radiative recombination processes. These devices exhibit several important applications: high-resolution gas spectroscopy, environmental contamination control, satellite communication and low loss IR fibers [3]. However, MCT single crystalline growth is very hard due to the physicochemical properties of this material. For example, a uniform composition of bulk MCT presents considerable difficulty because of segregation processes. Though many different materials have emerged as potential competitors, none of them exhibit such valuable properties as MCT [4].

The development of epitaxial growth techniques—VPE, LPE, MOCVD, MBE—have received considerable research efforts due to difficulties with ingot growth. CdTe is the usual substrate for MCT epitaxial growth but lately it

*Corresponding author. CINSO-CONICET-CITEFA, Juan Bautista de La Salle 4397, B1603ALO Villa Martelli, Pcia. de Bs. As., Argentina.
E-mail address: atrigubo@citefa.gov.ar (A.B. Trigubó).

0022-0248/$ - see front matter © 2006 Elsevier B.V. All rights reserved.
doi:10.1016/j.jcrysgro.2006.07.015

has been found that MCT grown on CdZnTe or CdTeSe shows better properties. This fact can be explained by the following:

- Ternary substrates exhibit a lower dislocation density than CdTe. Walukiewicz suggested that the alloying elements (Zn or Se) decrease the vacancy supersaturation in these materials immediately after solidification [5]. Then, the dislocation generation via vacancy condensation is partially inhibited. Moreover, Sher stated that the hardening effect of the alloying elements partly prevents dislocation generation and multiplication [6].
- Ternary substrates with the appropriate composition can match the MCT lattice parameter better than pure CdTe (Table 1). Hence, there is a lower misfit dislocation generation.

MCT epitaxial films grown on these substrates by MBE, LPE and MOCVD have been studied by other authors [7–9]. Nevertheless, those growth techniques are essentially different from the ISOVPE technique that was used in this work. Therefore, it is interesting to determine coincidences and differences in the results of ISOVPE-grown MCT. It can help towards a deeper comprehension of defect generation processes in this material and, as a consequence, to the design of control strategies to improve MCT's material properties. Even though ISOVPE is not a low-temperature epitaxial technique and therefore it is not a promising method for growing heterostructures or quantum wells for future generation of IR detectors, experience shows that this simple, low cost and versatile technique can be successfully used for a large variety of materials for IR devices [10].

The aim of this paper is to determine how the properties of ISOVPE-grown MCT epitaxial films were influenced by the substrate material (in our case, pure or alloyed CdTe) and their crystalline orientations.

2. Experimental procedure

Single-crystalline CdTe, $Cd_{0.96}Zn_{0.04}Te$ and $CdTe_{0.96}Se_{0.04}$ substrates with different crystallographic orientations [(1 1 1)Cd, (1 1 1)Te, (1 1 0), (1 0 0)] were employed. Commercial wafers from II–VI, Inc were used. The substrates were chemo-mechanically polished with Br_2 (1%) in an ethylene glycol solution using a CP3000 device from Logitech. The crystalline orientation was checked by X-ray diffraction (Laue technique) with a PW3710 Philips diffractometer.

A chemical etching was performed on each wafer, and the employed solutions were chosen according to their crystallographic orientation (Table 2). The dislocation density was measured on the micrographs of the etched substrates (Figs. 1–4). The misorientations between adjacent subgrains were evaluated using the Shockley–Read approximation (Table 3) [16].

The substrates were polished once again, as previously described, and epitaxial films were grown on them with the ISOVPE technique keeping source and substrate temperature at $(610 \pm 1)\,^{\circ}C$ without Hg overpressure. The growth time was 3.25 h. The epitaxial films were structurally characterized by X-ray diffraction. In every case, the single crystallinity and coincidence of the crystalline orientation between films and substrates were verified.

The surface morphologies of the films were examined by interference contrast using a metallographic optical microscope (Union Versamet) with Nomarski prism and polarized light. The thickness of films was also measured. The surface composition was analyzed with a Cameca microprobe in the wave dispersive mode and employing Cd, Zn, Te, and Se as standards; Hg was determined by the difference. The measurements of the dislocation density and adjacent subgrain misorientation of epitaxies were performed on the micrographs of the Hähnert-solution-etched films [15] (see Figs. 1–4 and Tables 2 and 3). The electrical properties (carrier density (p), resistivity (ρ) and

Table 1
Pure and alloyed substrates and MCT film ($x \cong 0.2$) lattice parameters

Material	CdTe	$Cd_{0.96}Zn_{0.04}Te$	$CdTe_{0.96}Se_{0.04}$	$Hg_{0.8}Cd_{0.2}Te$
Lattice parameter (Å)	6.4823	6.4656	6.4649	6.4637

Table 2
Composition of etching solutions used and the respective crystallographic plane revealed

Etchant	Etchant chemical composition	Revealed planes
Nakagawa et al. [11]	3HF: $2H_2O_2$: $2H_2O$	(1 1 1)Cd
Bagai et al. [12]	4HF: $0.5H_2O_2$: $2H_2O$	(1 1 1)Te
Inoue et al. [13]	20 ml H_2O + 4 g $K_2Cr_2O_7$ + 10 ml HNO_3 + 1.5 mg NO_3Ag	(1 1 0)
Wermke et al. [14]	1HF: $3HNO_3$: $4AgNO_3$ 1%	(1 0 0)
Hähnert et al. [15]	1{1HF: $1CrO_3$ 50%: 1ClH} + $8H_2O$	All the above reported MCT planes.

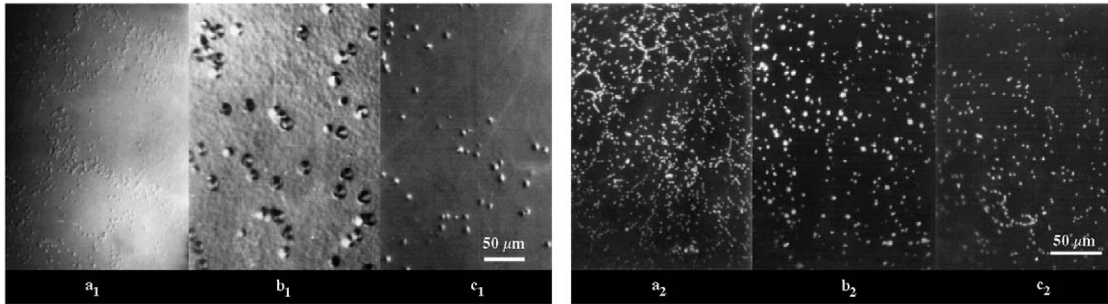

Fig. 1. Crystallographic orientation (1 1 1)Cd. (a_1) Chemical etching of the pure CdTe substrate. (a_2) Chemical etching of the epitaxial film grown on the pure CdTe substrate (a_1). (b_1) Chemical etching of the $CdTe_{0.96}Se_{0.04}$ substrate. (b_2) Chemical etching of the epitaxial film grown on the $CdTe_{0.96}Se_{0.04}$ substrate (b_1). (c_1) Chemical etching of the $Cd_{0.96}Zn_{0.04}Te$ substrate. (c_2) Chemical etching of the epitaxial film grown on the $Cd_{0.96}Zn_{0.04}Te$ substrate (c_1).

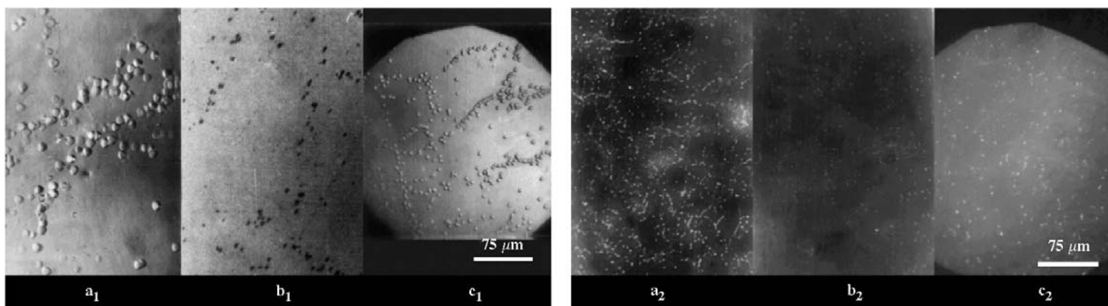

Fig. 2. Crystallographic orientation (1 1 1)Te. (a_1) Chemical etching of the pure CdTe substrate. (a_2) Chemical etching of the epitaxial film grown on the pure CdTe substrate (a_1). (b_1) Chemical etching of the $CdTe_{0.96}Se_{0.04}$ substrate. (b_2) Chemical etching of the epitaxial film grown on the $CdTe_{0.96}Se_{0.04}$ substrate (b_1). (c_1) Chemical etching of the $Cd_{0.96}Zn_{0.04}Te$ substrate. (c_2) Chemical etching of the epitaxial film grown on the $Cd_{0.96}Zn_{0.04}Te$ substrate (c_1).

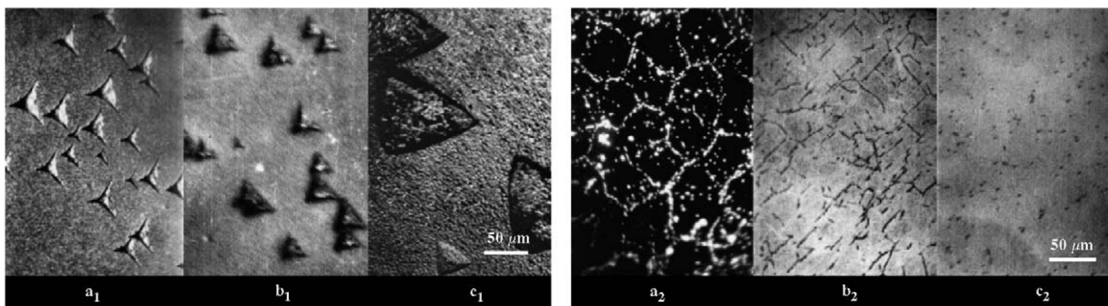

Fig. 3. Crystallographic orientation (1 1 0). (a_1) Chemical etching of the pure CdTe substrate. (a_2) Chemical etching of the epitaxial film grown on the pure CdTe substrate (a_1). (b_1) Chemical etching of the $CdTe_{0.96}Se_{0.04}$ substrate. (b_2) Chemical etching of the epitaxial film grown on the $CdTe_{0.96}Se_{0.04}$ substrate (b_1). (c_1) Chemical etching of the $Cd_{0.96}Zn_{0.04}Te$ substrate. (c_2) Chemical etching of the epitaxial film grown on the $Cd_{0.96}Zn_{0.04}Te$ substrate (c_1).

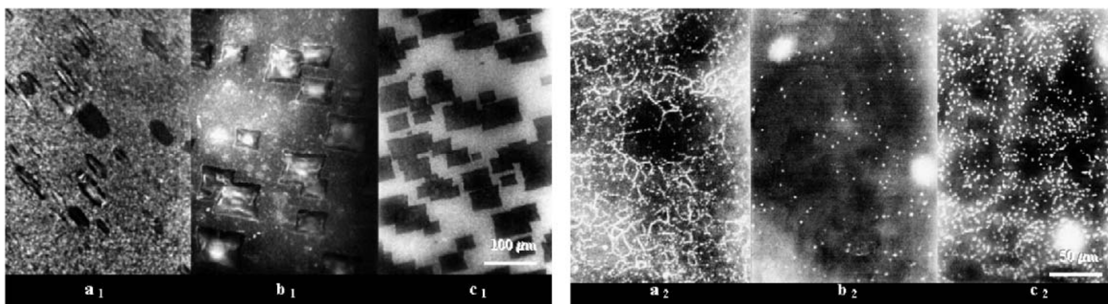

Fig. 4. Crystallographic orientation (1 0 0). (a_1) Chemical etching of the pure CdTe substrate. (a_2) Chemical etching of the epitaxial film grown on the pure CdTe substrate (a_1). (b_1) Chemical etching of the $CdTe_{0.96}Se_{0.04}$ substrate. (b_2) Chemical etching of the epitaxial film grown on the $CdTe_{0.96}Se_{0.04}$ substrate (b_1). (c_1) Chemical etching of the $Cd_{0.96}Zn_{0.04}Te$ substrate. (c_2) Chemical etching of the epitaxial film grown on the $Cd_{0.96}Zn_{0.04}Te$ substrate (c_1).

Table 3
Crystallographic orientation, dislocation density ($\delta_{\perp}$), and subgrain misorientation (φ) for the pure and alloyed substrates

Substrates					Epitaxial Films				
Material	Crystall Orient.	$\delta_{\perp}$ (cm^{-2})	φ (“)	Fig. no.	Thickness (μm)	$\langle x \rangle$	$\delta_{\perp}$ (cm^{-2})	φ (“)	Fig. no.
CdTe	(1 1 1)Cd	4.3×10^{5}	19	1a$_1$	25	0.18	2.2×10^{6}	80	1a$_2$
$Cd_{0.96}Zn_{0.04}Te$.	(1 1 1)Cd	1.1×10^{5}	19	1b$_1$	40	0.22	5.3×10^{5}	17	1b$_2$
$CdTe_{0.96}Se_{0.04}$	(1 1 1)Cd	7.8×10^{4}	6	1c$_1$	25	0.18	5.2×10^{5}	14	1c$_2$
CdTe	(1 1 1)Te	1.2×10^{5}	8	2a$_1$	28	0.23	1.1×10^{6}	43	2a$_2$
$Cd_{0.96}Zn_{0.04}Te$	(1 1 1)Te	7.0×10^{4}	6	2b$_1$	29	0.19	4.4×10^{5}	15	2b$_2$
$CdTe_{0.96}Se_{0.04}$	(1 1 1)Te	5.0×10^{4}	3	2c$_1$	26	0.20	8.0×10^{5}	40	2c$_2$
CdTe	(1 1 0)	4.0×10^{4}	4	3a$_1$	30	0.23	6.0×10^{6}	85	3a$_2$
$Cd_{0.96}Zn_{0.04}Te$	(1 1 0)	4.9×10^{3}	4	3b$_1$	25	0.20	8.0×10^{5}	21	3b$_2$
$CdTe_{0.96}Se_{0.04}$	(1 1 0)	2.0×10^{4}	4	3c$_1$	30	0.20	5.0×10^{6}	98	3c$_2$
CdTe	(1 0 0)	2.0×10^{5}	17	4a$_1$	26	0.23	3.4×10^{6}	65	4a$_2$
$Cd_{0.96}Zn_{0.04}Te$	(1 0 0)	2.1×10^{4}	3	4b$_1$	27	0.29	1.0×10^{6}	32	4b$_2$
$CdTe_{0.96}Se_{0.04}$	(1 0 0)	1.0×10^{4}	2	4c$_1$	25	0.27	3.2×10^{5}	10	4c$_2$

Thickness, average surface composition, dislocation density ($\delta_{\perp}$), and subgrain misorientation (φ) of the corresponding epitaxial MCT films grown on the different substrates.

Table 4
Crystallographic orientation of the pure and alloyed substrates

Substrates		Epitaxial films		
Material	Crystall Orient	Hall effect measurements (77 K)		
		p (cm^{-3})	ρ (Ω cm)	μ (cm^2 V^{-1} s^{-1})
CdTe	(1 1 1)Cd	2.8×10^{16}	5.9×10^{-2}	3785
$Cd_{0.96}Zn_{0.04}Te$.	(1 1 1)Cd	2.6×10^{17}	2.5×10^{-2}	950
$CdTe_{0.96}Se_{0.04}$	(1 1 1)Cd	1.5×10^{17}	5.1×10^{-2}	839
CdTe	(1 1 1)Te	2.0×10^{18}	9.0×10^{-3}	316
$Cd_{0.96}Zn_{0.04}Te$	(1 1 1)Te	1.0×10^{17}	9.0×10^{-2}	645
$CdTe_{0.96}Se_{0.04}$	(1 1 1)Te	5.0×10^{17}	4.6×10^{-2}	250
CdTe	(1 1 0)	1.7×10^{19}	9.0×10^{-3}	42
$Cd_{0.96}Zn_{0.04}Te$	(1 1 0)	5.7×10^{16}	2.0×10^{-1}	462
$CdTe_{0.96}Se_{0.04}$	(1 1 0)	2.5×10^{18}	6.0×10^{-3}	418
CdTe	(1 0 0)	5.9×10^{17}	1.4×10^{-2}	563
$Cd_{0.96}Zn_{0.04}Te$	(1 0 0)	3.6×10^{18}	1.4×10^{-2}	119
$CdTe_{0.96}Se_{0.04}$	(1 0 0)	3.3×10^{17}	6.5×10^{-2}	290

Electrical properties of the corresponding epitaxial MCT films grown on the different substrates.

carrier mobility (μ)) were evaluated using Hall effect measurements at 77 K, which is the usual operating temperature for detectors (Table 4).

3. Discussion

The quality of MCT IR detectors is influenced by the purity of the material and the growth process conditions. Some of the most important material characteristics determined by the growth method are composition homogeneity, point defect concentration, dislocation density and distribution and surface morphology.

The films have a good compositional homogeneity over their entire surface ($\Delta x = 0.01$). This fact makes them have a homogeneous responsivity to the same infrared wavelength range (Table 3).

The point defect concentration, mainly Hg vacancies, determine the carrier density. MCT can be grown by the ISOVPE technique either with or without Hg overpressure. In the latter case the Hg vacancy concentration is higher, hence the hole concentration is higher as well [17]. In Table 4 it can be seen that the hole concentration is in the range of 10^{17}–10^{18} cm^{-3}. In MCT grown with Hg overpressure, the hole concentration frequently has a value of $\sim10^{16}$ cm^{-3}.

Most of the carrier mobility values are in the range of 400–800 cm^2 V^{-1} s^{-1} (Table 4), similar to values found in Ref. [2,18] even though some of them exhibit higher dispersion. As there is no correlation between carrier mobility and dislocation density data, only contamination during the growth process could be responsible for the carrier mobility fluctuations due to the initial homogeneity in purity level of substrates and source material (HgTe). Coincidentally with other authors [2] who have experimentally studied the phenomena, impurity scattering is the likely mechanism that limits the carrier mobility.

Dislocations are electrically active in MCT and can influence the radiative recombination processes, which can adversely affect the carrier lifetime [19]. Consequently, it is important to know the dislocation density and distribution. The results shown in Table 3 give rise to the following considerations:

- The dislocation densities ($\delta_{\perp}$) of the epitaxial film are larger than the dislocation densities ($\delta_{\perp}$) of the substrates.
- The dislocation densities ($\delta_{\perp}$) of the epitaxial films grown on the alloyed substrates are lower than the dislocation densities ($\delta_{\perp}$) of the epitaxial films grown on pure CdTe.
- The ratio of the epitaxial $\delta_{\perp}$ to the substrate $\delta_{\perp}$ exhibits similar values for the (1 1 1)Cd and (1 1 1)Te orientations, but they are lower than the values found for the (1 1 0) and (1 0 0) orientations. Probably, these differences are due to the different qualities of the chemical etchants. Hähnert for epitaxies [15] and Nakagawa et al. [11] and Bagai et al. [12], respectively for (1 1 1)Cd and (1 1 1)Te substrates, are reliable chemical etchants. In spite of not being considered as reliable chemical etchants, the Inoue [13] solution for (1 1 0) substrates and Wermke et al. [14] solution for (1 0 0) substrates are usually used, since there are no other known etchants for these purposes [20–22].

The dislocation distribution on CdTe substrates has a well-defined subgrain structure. This is not so on CdZnTe and CdTeSe substrates. The subgrain structure could only be observed on the (1 1 1)Cd and (1 1 1)Te crystallographic orientations due to the mentioned characteristics of the used chemical etchants. The latter reason also revealed large etch pits and a low substrate dislocation density on the (1 1 0) and (1 0 0) crystal planes (Figs. 1–4).

A well-defined substrate subgrain structure, as always observed in CdTe, also defines a similar ISOVPE MCT epitaxy subgrain structure. Adverse electrical effects of dislocations in subgrain borders [23] can be prevented using ternary substrates for MCT epitaxial films.

Chemical etching of the epitaxial films grown on (1 0 0)CdTe (Fig. $4a_2$) and (1 1 0)CdTeSe (Fig. $3b_2$) revealed unresolved etch pits that appeared as short segments or curved lines on the micrographs. These have been attributed to the presence of tellurium precipitates that generated localized stress and dislocations. These precipitates only show up for growth conditions where there is no Hg overpressure [18].

Surface morphological defects can act as crystalline defect sources, and they are associated with local compositional variations [24]. ISOVPE MCT films show that the surface morphology is independent of substrates for both pure and alloyed substrates, but it is different for each crystalline orientation [25–27]. In Figs. 5b–d it can be observed that epitaxial morphology is slightly dependent on misorientation with regard to (1 1 1)Te, (1 1 0) and (1 0 0) crystallographic planes, showing that the epitaxy edges have a similar morphology to that of the central

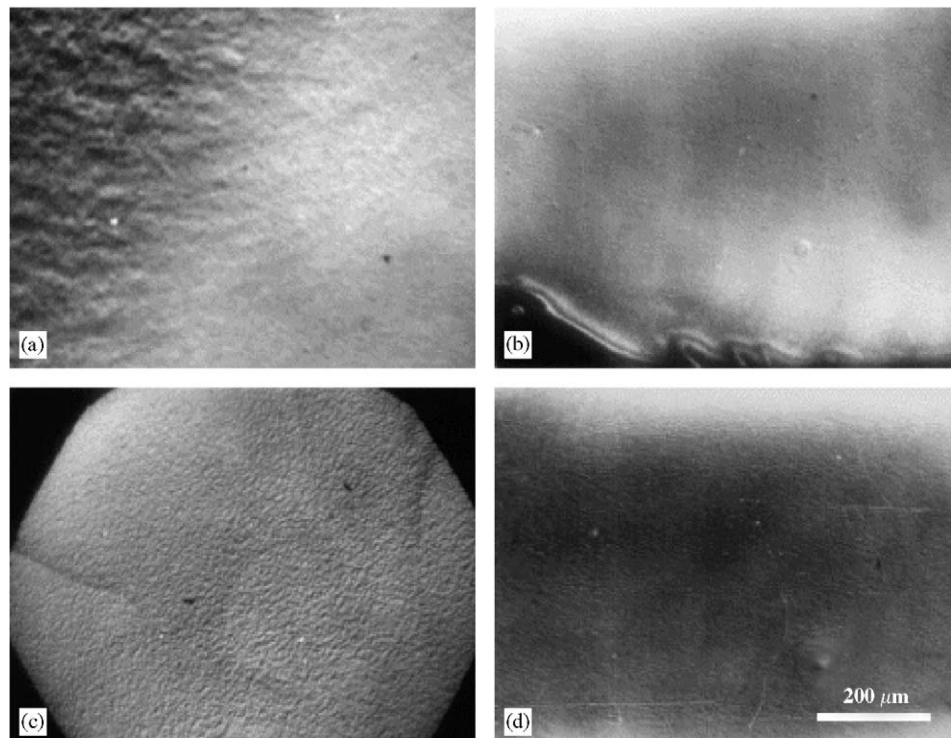

Fig. 5. Morphology of the epitaxies grown on different crystallographic orientations. (a) (1 1 1)Cd MCT film grown on $CdTe_{0.96}Se_{0.04}$ substrate. (b) (1 1 1)Te MCT film grown on pure CdTe substrate. (c) (1 1 0) MCT film grown on CdTe substrate. (d) (1 0 0) MCT film grown on $CdTe_{0.96}Se_{0.04}$ substrate.

zone. The previously mentioned misorientation is produced by the polishing process. Meanwhile, in the (1 1 1)Cd epitaxial films (Fig. 5a), the morphology is strongly dependent on misorientations with regard to the (1 1 1)Cd direction.

It has been found, in agreement with Stevenson et al. [28,29], that the film thickness and surface chemical composition are independent of the crystalline orientation (Table 3). These facts were experimentally supported by the linear relation between film thickness and the square root of time showing a diffusive-controlled process [30–36]. Besides, this experimental evidence can be explained by the Djuric model over the wide temperature and pressure range used in the ISOVPE MCT growth, which is indicative of a diffusion-limited process [37].

Since diffusive control is independent of crystal polarity, this fact could not explain the morphological differences between the epitaxial films for the crystallographic orientations (1 1 1)Cd (Fig. 5a) and (1 1 1)Te (Fig. 5b) [28,29]. The observed differences probably can be attributed to the initial growth stages where kinetic control could be determined by the surface phenomena, in which crystal structure and surface order have an important role for each crystallographic orientation. The consequence is that each crystalline plane has a different growth rate, giving rise to a dissimilar ripple generation [24] (see Fig. 5).

4. Conclusions

- The electrical properties of MCT epitaxial films grown on the different substrates with different crystallographic orientations are remarkable and comparable to other values reported in the technical literature.
- The epitaxial films grown on the ternary substrates exhibit a lower dislocation density. This fact could determine a larger carrier lifetime and, consequently, better electrical properties for devices.
- The surface morphology of MCT epitaxial films only depends on the crystallographic orientation, being independent of the use of a pure or alloyed substrate. It is also independent of a low misorientation with regard to the chosen crystallographic orientation with the exception of the (1 1 1)Cd growth direction. These experimental facts have practical importance as the ISOVPE technique enables a better exploitation of the substrate ingots, just as the use of cheaper CdTe enabled the manufacture of less sophisticated IR devices.

Acknowledgments

The authors are indebted to CONICET for Grant no. 403/97, which allowed for the research results.

References

[1] C.T. Elliot, Electron. Lett. 17 (1981) 312.
[2] P. Capper (Ed.), Narrow-Gap Based Compounds, Emis Datarewiews Series No. 10, INSPEC, 1994.
[3] Y. Horikoshi, Semicond. Semimet. 22c (1985) 93.
[4] A. Rogalski, New Ternary Alloy Systems for Infrared Detectors, SPIE Optical Engineering Press, 1994 (pp. 1–3).
[5] W. Walukiewicz, Appl. Phys. Lett. 54 (1989) 2009.
[6] A. Sher, A.B. Chen, W.E. Spicer, Appl. Phys. Lett. 46 (1985) 54.
[7] R.F.C. Farrow, J. Vac. Sci. Technol. A 3 (1985) 60.
[8] Y. Nemirovsky, S. Margalit, E. Finkman, Y. Shachman-Diamand, I. Kidron, J. Electron. Mater. 11 (1982) 133.
[9] P.Y. Lu, L.M. Williams, C.H. Wang, S.N.G. Chu, J. Vac. Sci. Technol. A 5 (1987) 3153.
[10] K. Adamiec, M. Grudzien, Z. Nowak, J. Pawluczyk, J. Piotrowski, J. Antoszewski, J. Dell, C. Musca, L. Faraone, Proceedings of SPIE 2999 (1997) 34.
[11] K. Nakagawa, K. Maeda, S. Takeuchi, Appl. Phys. Lett. 34 (9) (1979) 574.
[12] R. Bagai, G. Mohan, L. Seth, W.N. Borle, J. Crystal Growth 85 (1987) 386.
[13] M. Inoue, Y. Teramoto, S. Takanayagi, J. Appl. Phys. 33 (1962) 2578.
[14] B. Wermke, N. Muhlberg, Cryst. Res. Technol. 24 (1989) 365.
[15] I. Hähnert, M. Schenk, J. Crystal Growth 101 (1990) 251.
[16] J.P. Hirth, J. Lothe, Theory of Dislocations, McGraw-Hill, New York, 1968.
[17] H.R. Vydyanath, J. Vac. Sci. Technol. B 9 (1991) 1716.
[18] A.B. Trigubó, Ph.D. thesis, Buenos Aires University, Argentina, 1992.
[19] T.H. Moore, H.F. Schaake, J. Vac. Sci. Technol. A 1 (1983) 1666.
[20] U. Gilabert, A.B. Trigubó, N.E. Walsöe de Reca, J. Mater. Sci. Eng. B 27 (1994) L11.
[21] U. Gilabert, A.B. Trigubó, N.E. Walsöe de Reca, Ann. Assoc. Quím. Argent. 83 (1–2) (1995) 73.
[22] U. Gilabert, A.B. Trigubó, G.E. Lascalea, N.E. Walsöe de Reca, Defect Diffus. Forum 152 (1997) 27.
[23] D.J. Williams, A.W. Vere, J. Crystal Growth 83 (1987) 341.
[24] G. Cinader, A. Raizman, A. Sher, J. Vac. Sci. Technol. B 9 (3) (1991) 1634.
[25] A.B. Trigubó, N.E. Walsöe de Reca, Mater. Sci. Eng. B 27 (1994) 87.
[26] M.H. Aguirre, H.R. Cánepa, U. Gilabert, E.A. Heredia, A.B. Trigubó, N.E. Walsöe de Reca, Recent Res. Dev. Crystal Growth 3 (2003) 61 (Chapter 4; transworld research network).
[27] M.C. Di Stefano, E. Heredia, U. Gilabert, A.B. Trigubó, Cryst. Res. Technol. 39 (10) (2004) 881.
[28] J.G. Fleming, D.A. Stevenson, J. Vac. Sci. Technol. A 5 (1987) 3383.
[29] J.G. Fleming, D.A. Stevenson, Phys. Stat. Sol. 105 (1987) 77.
[30] N. Tufte, E. Stelzer, J. Appl. Phys. 40 (1969) 4559.
[31] J.G. Fleming, D.A. Stevenson, J. Crystal Growth 82 (1987) 621.
[32] Y. Nemirovsky, A. Kepten, J. Electron. Mater. 13 (1984) 867.
[33] G. Attolini, O. De Melo, F. Lecabbue, R. Panizzieri, C. Pelosi, Mater. Lett. 8 (1989) 313.
[34] L. Svob, Y. Marfaing, R. Triboulet, F. Bailly, G. Cohen-Solal, J. Appl. Phys. 46 (1975) 4521.
[35] M. Isshiki, Y. Maruyama, S. Tobe, Jpn. J. Appl. Phys. 31 (1992) 1842.
[36] B. Koo, J. Wang, Y. Ishikawa, Ch.G. Lee, M. Isshiki, Jpn. J. Appl. Phys. 37 (9A) (1998) 4914 (Pt. 1).
[37] E. Moyano, A. Scarpettini, U. Gilabert, A.B. Trigubó, Thin Solid Films 373 (1–2) (2000) 28.